Chapter 7

Effects of Isovalent Substitutions and Heat Treatments on T_c, Orthorhombicity, Resistivity, AC Magnetic Shielding and Irreversibility Line in High-T_c Superconductors

Abdelhakim Nafidi

Additional information is available at the end of the chapter

http://dx.doi.org/10.5772/intechopen.74354

Abstract

We report here the preparation, X-ray diffraction with Rietveld refinement, AC magnetic susceptibility ($\chi_{ac} = \chi' + i\chi''$), resistivity, iodometric measurements and effect of heat treatments in $(Y_{1-x}Sm_x)SrBaCu_3O_{6+z}$. Each sample has undergone two types of heat treatment: oxygen annealing [O] and argon annealing followed by oxygen annealing [AO]. For each x, the [AO] heat treatment increases the orthorhombicity $\varepsilon = (b - a)/(b + a)$ (for $0 \le x \le 1$), T_c (for $x \ge 0.4$) and reduced the linear resistivity parameters with a diminution of the interaction of holes with phonons. At all $T < T_c$ and for any applied field H_{dc}, we observed an enhancement of AC magnetic shielding and the irreversibility line in the samples [AO] for $x > 0.5$, revealing an improvement in the pinning properties. Remarkable correlations were found. In the [AO] samples, the measured data are explained by the increase in phase purity, in cationic and chain oxygen ordering, p_{sh} and the decrease in d[Cu(1)—(Sr/Ba)].

Keywords: chain oxygen order-disorder, heat treatments control of T_c, Rietveld refinement structure, phase transition, irreversibility line, AC magnetic shielding, resistivity, $(Y_{1-x}Sm_x)(SrBa)Cu_3O_{6+z}$ type-II superconductors

1. Introduction

$YBa_2Cu_3O_{6.95}$ is superconducting below 92 K and characterized by double $Cu(2)O_2$ layers (oriented along the a-b plane) responsible for carrying the supercurrent and Cu(1)O chains (along the b direction) that provide a charge reservoir for these planes [1, 2].

The four distinct crystallographic sites Y, Ba, Cu plane, and Cu chain can be substituted with different elements. Single-phase $LnBa_2Cu_3O_{6+z}$ (Ln = rare earth) can be synthesized with T_c = 92 K. All these compounds show an orthorhombically distorted oxygen-deficient triple-perovskite structure and both the orthorhombic distortion and T_c depend sensitively on the oxygen content (6 + z) [3]. Wada et al. [4], Izumi et al. [5] studied the structural and superconducting properties of $La_{1+x}Ba_{2-x}Cu_3O_y$ (with $0 \leq x \leq 0.5$). They concluded that in order to have T_c maximal, this structure must have an ordered arrangement of La and Ba along c axis with an occupation factor of 0 and 1 for the oxygen at (1/2, 0, 0) and (0, 1/2, 0), respectively.

We want to see if an isovalent substitution of Ba^{+2} by Sr^{+2} with smaller ionic radius can modify the results discussed above when Y^{+3} is replaced by the rare earth Sm^{+3} with bigger ionic radius. Understanding the effect of the Y and Ba atomic plans on the superconductivity in these compounds, we have studied the structural, superconducting and magnetic properties of $(Y_{1-x}Sm_x)SrBaCu_3O_{6+z}$. We found that the effect of heat treatments on these properties depended on the content of Sm.

2. Experimental techniques

We prepared the polycrystalline samples by solid-state sintering of oxides (Y_2O_3, Sm_2O_3, CuO) with a purity of 99.999% and carbonates ($SrCO_3$ 99.999% pure, $BaCO_3$ with a purity of 99.99%). All these chemicals were thoroughly mixed in desired proportions and calcined at 950°C in air for 12–18 h. The obtained ceramic was ground, mixed, pelletized and heated in air at 980°C for 16–24 h. This was repeated twice. For each sample, the circular pellets were subjected to heat treatment in oxygen at 450°C for 60–72 h and furnace cooled. This was denoted as sample [O].

X-ray diffraction spectra of the samples were measured with Philips diffractometer fitted with a secondary beam graphite monochromator and using Cu Kα (40 kV/20 mA) radiation. The angle 2θ was varied from 20° to 120° in steps of 0.025°and the counting time per step was 10 s. The XRD spectra were resolved with Rietveld refinement.

A detailed description of the basic arrangement of the experiment of the AC magnetic susceptibility can be found in [6]. The sample in the form of a slab is placed in the magnetic field $H_{ext} = H_{dc} + H_{ac}\cos(\omega t)$ with the static component H_{dc} and the AC component with the amplitude H_{ac} and the frequency $f = \omega/2\pi$. The sample's magnetic response was detected by a pick-up coil surrounding the sample. Superconducting transitions were determined by the measure of the real (χ') and the imaginary (χ'') parts of the AC magnetic susceptibility as a function of temperature in H_{ac} = 0.11 Oe and at f = 1500 Hz. Also, χ' and χ'' were measured in $0 < H_{dc} < 150$ Oe with applied H_{ac}.

We used the Van Der Pauw method [7] for measuring resistivity $\rho(T)$. The sample was attached to a cane in a cryostat with closed helium circuit with a cryogenic pump, a regulator of temperature (1 μA–10 mA) and 1 μV resolution digital voltmeter controlled with a computer. T_c was determined by both the measured $\chi'(T)$ and $\rho(T)$.

For each x, the same sample [O] was then heated in argon at 850°C for about 12 h, cooled to 20°C and oxygen was allowed to flow instead of argon and the sample was annealed at 450°C

http://dx.doi.org/10.5772/intechopen.74354

for about 72 h. This sample is denoted as [AO]. XRD, resistivity and AC susceptibility measurements were done on a part of this sample. We measured 6 + z by iodometry technique on a part of each sample.

3. Results

3.1. Crystalline structure

The X-ray diffraction spectra of all the samples are shown in **Figure 1** [8]. After the [AO] heat treatment, the reflections were sharper so the samples were well crystallized. The [AO] heat treatment increases the orthorhombic cleaving. For example, the (123) and (213) peaks at 2θ ≈ 58.5° (and (200) and (006) reflections at 2θ ≈ 47°) which were ill-resolved for the [O] samples were clearly identified after the [AO] heat treatment, as shown in **Figure 1**. Some weak unidentified impurity peaks (marked by crosses in **Figure 1(a)** were seen in the [O] samples and their amplitudes increase with x. They disappeared after the [AO] treatment shown in **Figure 1(b)**. This indicates an improvement of crystallographic quality of the samples [AO].

In **Figure 2** we show, respectively, the variation of the parameters a, b, c and the volume V of the unit cell obtained with Rietveld refinement [9] as a function of x and heat treatment. When x increases, the lattice parameter a (c and the volume V of the unit cell) increased but b is constant leading to a decrease of the orthorhombicity (ε = (b − a)/(b + a)) ε [O] in **Figure 3**. The substitution of Y^{+3} (0.893 Å) by the rare earth Sm^{+3} (0.965 Å), with a superior ionic radius, leads to a linear increase of c and V.

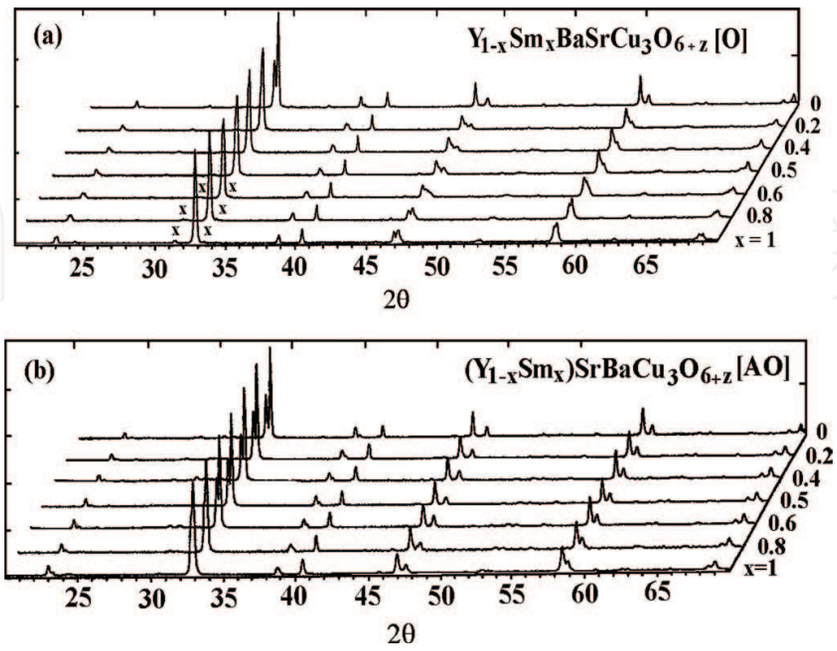

Figure 1. XRD (Cu Kα) patterns of $(Y_{1-x}Sm_x)SrBaCu_3O_{6+z}$ as a function of x. (a) Samples [O] annealed in oxygen at 450°C, (b) samples [AO] heated in argon at 850°C followed by annealing in oxygen at 450°C (x = impurity peaks).

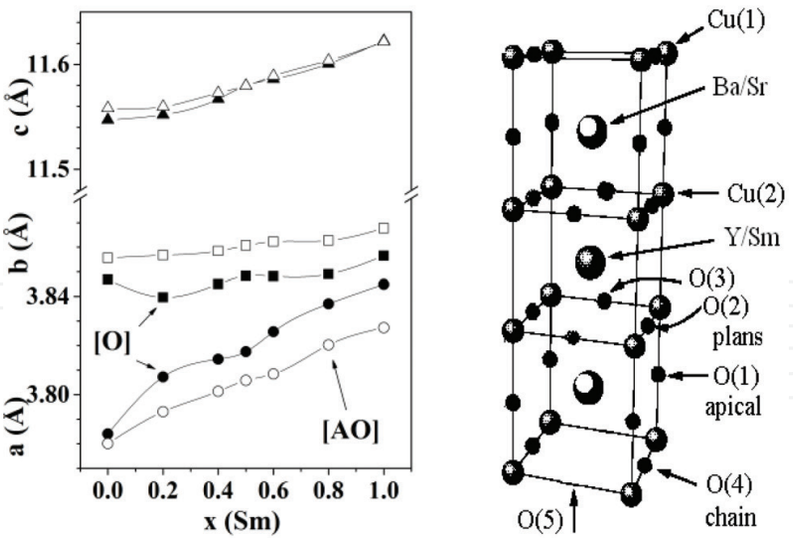

Figure 2. Variation of the parameters a, b and c of $(Y_{1-x}Sm_x)SrBaCu_3O_{6+z}$ as a function of x and heat treatment in the left. The unit cell of $(Y_{1-x}Sm_x)SrBaCu_3O_{6+z}$ in the right.

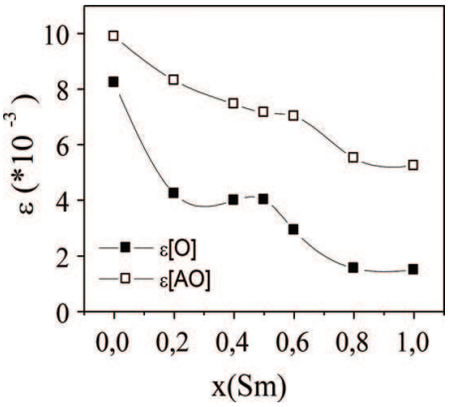

Figure 3. Variation of the orthorhombicity of $(Y_{1-x}Sm_x)SrBaCu_3O_{6+z}$ as a function of x and heat treatment.

The orthorhombicity depends strongly on the Sm content x. When x increases from 0 to 1, ε decreases quickly from 8.24×10^{-3} to 1.5×10^{-3} in the samples [O] in **Figure 3**. This indicated a structural phase transition from orthorhombic to tetragonal. ε decreases slowly from 9.9×10^{-3} to 5.24×10^{-3} with an orthorhombic symmetry in the samples [AO]. We found also that the orthorhombicity depends strongly on the heat treatment [AO]. For each x, the latter increased the orthorhombicity (for $0 \leq x \leq 1$). The increase was maximum, from 1.5×10^{-3} to 5.24×10^{-3} for x = 1 in [12].

3.2. Real part of the AC magnetic susceptibility and T_c

The critical temperature T_c of the transition from the superconductor to the normal state depends strongly on the effect of [AO] heat treatment as seen in the real part of AC susceptibility $\chi'(T)$ in **Figure 4**. The imaginary part of AC susceptibility $\chi''(T)$ in **Figure 4** shows a single peak T_p. This defined clearly the value of T_c for all the samples. We can see in **Figure 5** that when x was increased from 0 to 1, T_c[O] decreased from 83 K to 79.3 K. T_c[AO] first decreases

http://dx.doi.org/10.5772/intechopen.74354

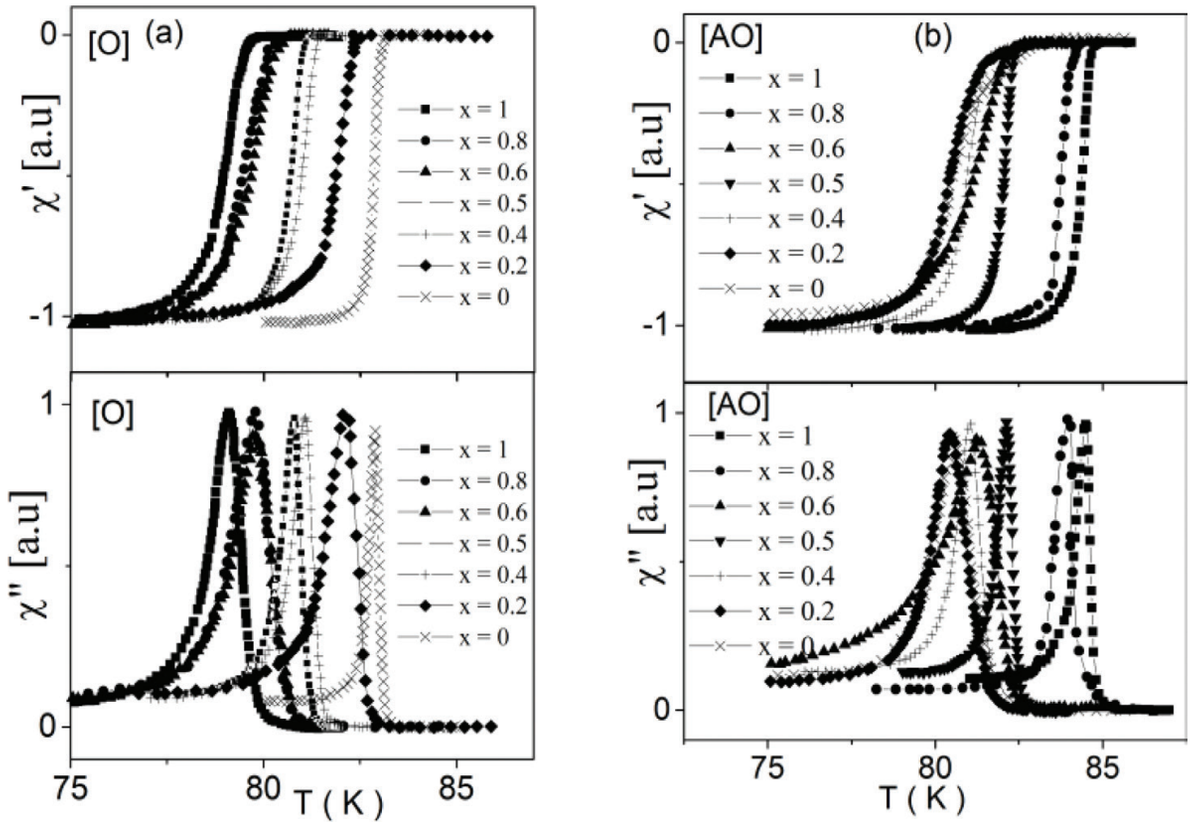

Figure 4. χ' and χ'' of $(Y_{1-x}Sm_x)SrBaCu_3O_{6+z}$ as a function of temperature. (a) Heat treatment [O], (b) heat treatment [AO].

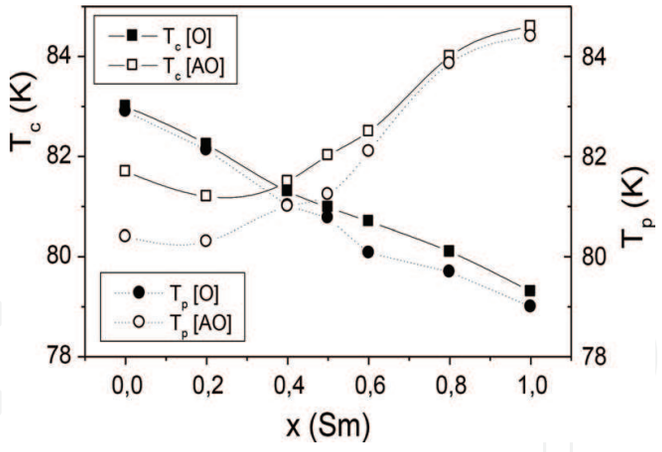

Figure 5. T_c and T_p of $(Y_{1-x}Sm_x)SrBaCu_3O_{6+z}$ as a function of x(Sm) following the [O] and [AO] heat treatments.

from 81.7 K (for x = 0) to 81.2 K (for x = 0.2) (like in the samples [O]) and then increases to 85 K for $SmSrBaCu_3O_{6+z}$. For each x, the [AO] heat treatment increases T_c for $x \geq 0.4$ and decreases it for $x < 0.4$. A maximum of increase in T_c of 6 K was observed in $SmSrBaCu_3O_{6+z}$ [AO] [8].

For each x, the [AO] heat treatment increases ε (for $0 \leq x \leq 1$) in **Figure 3** and T_c (for $x \geq 0.4$) in **Figure 5**. The [AO] heat treatment makes the coupling of the superconducting grains by Josephson junctions took place at higher temperature. This effect is revealed by the net displacement of T_p to higher temperature for $x \geq 0.4$.

x	0		0.2		0.4		0.5		0.6		0.8		1	
Heat treatment	**[O]**	**[AO]**	**[O]**	**[AO]**	**[O]**	**[AO]**	**[O]**	**[AO]**	**[O]**	**[AO]**	**[O]**	**[AO]**	**[O]**	**[AO]**
a (Å)	3.846	3.855	3.839	3.856	3.845	3.858	3.848	3.860	3.848	3.862	3.849	3.862	3.856	3.867
b (Å)	3.784	3.780	3.807	3.793	3.814	3.801	3.817	3.805	3.825	3.808	3.837	3.820	3.844	3.827
c (Å)	11.55	11.56	11.55	11.56	11.57	11.57	11.58	11.58	11.59	11.59	11.60	11.60	11.62	11.62
V (Å)	168.0	168.4	168.8	169.0	169.6	169.7	170.1	170.1	170.5	170.4	171.3	171.1	172.3	172.0
ε (10^{-3})	8.24	9.90	4.24	8.32	3.99	7.46	4.02	7.16	2.93	7.02	1.56	5.52	1.50	5.24
T_c (K)	83	81.7	82.24	81.2	81.3	81.5	81	82.02	80.7	82.5	80.1	84	79.3	84.6
T_p (K)	82.9	80.4	82.13	80.3	81.02	81	80.77	81.24	80.07	82.1	79.7	83.86	79	84.4
ΔT_c	0.4	0.41	1.42	2	1.1	1	0.92	0.8	1.7	2.9	1.58	0.72	1.5	0.8
ΔT_p	0.3	1.2	0.89	1.3	0.7	0.9	0.65	0.56	1.2	2.2	1.05	0.56	0.96	0.51
K′ (Oe)	—	—	2068	3390	1679	3848	1447	5177	1057	5910	936	8165	1677	11,741
n	—	—	1.41	1.50	1.33	1.53	1.13	1.88	1.14	1.63	0.91	1.54	1.31	1.33

Table 1. Structural, superconducting and magnetic parameters of $(Y_{1-x}Sm_x)SrBaCu_3O_{6+z}$.

http://dx.doi.org/10.5772/intechopen.74354

Table 1 shows the exact measured values of the structural parameters a, b, c, V and ε of each sample as a function of the heat treatment.

3.3. Real part of the AC magnetic susceptibility and the shielding effect

The effect of [AO] heat treatment on T_c was remarkable. The temperature at which the diamagnetism sets in is taken as T_c and it was found to be dependent on both x and the heat treatment employed. Since the same sample was used for both heat treatments, one can compare the diamagnetic response and note that screening current of the [AO] sample increased considerably compared to that of the [O] sample for each x (see, for example, the case x = 0.8 in **Figure 6(a)**). **Table 1** shows the exact measured values of the superconducting parameters T_c, T_p, ΔT_c and ΔT_p of each sample as a function of the heat treatment.

We can see in **Figure 7** the shielding effect S which is the amplitude of the real part of the AC susceptibility [10–12]. S represents the exclusion of the magnetic flux by the sample in alternative dynamic mode. S was set arbitrarily equal to 0.89, 0.97 and 1, respectively, for x = 0.5, 0.8, and 1, for the sample [AO] at 55 K and for H_{dc} = 0 Oe.

For each x > 0.5, the [AO] heat treatment increases the shielding effect at all $T < T_c$ and for any applied H_{dc}. For example, in $SmSrBaCu3O_{6+z}$ (x = 1), S[AO] = 2 S[O] at T = 65 K and H_{dc} = 126.5 Oe [13]. When H_{dc} increases, S[AO] decreases slowly than S[O]. For example, at T = 55 K, S[AO] decreases by 10% whereas S[O] decreases by 70%. This indicated an improvement of the quality of the grains and intergranular coupling in the samples [AO].

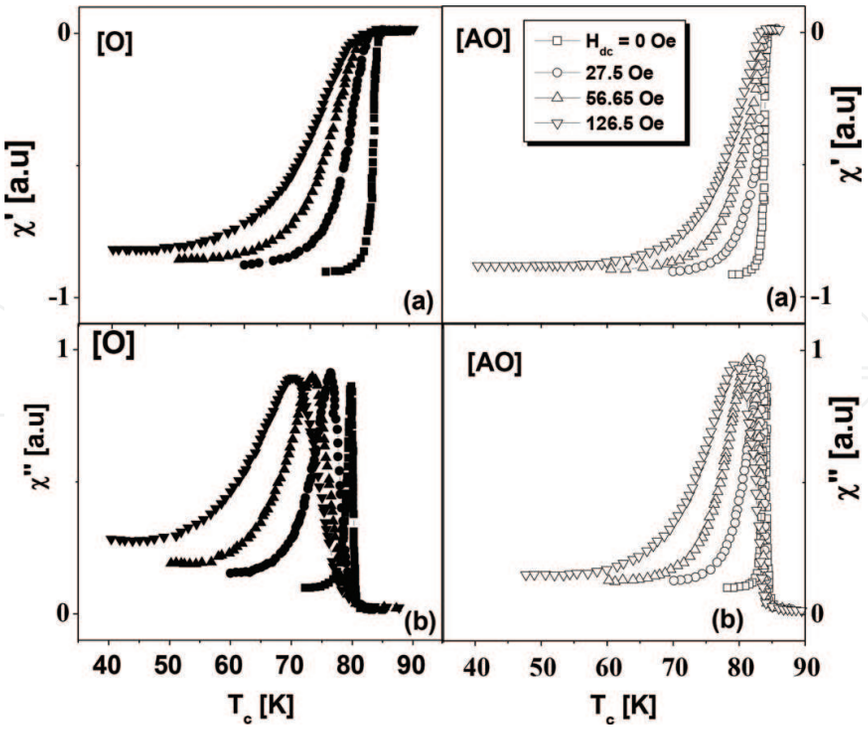

Figure 6. (a) χ′ and (b) χ″ of $(Y_{0.2}Sm_{0.8})SrBaCu_3O_{6+z}$ as a function of the temperature and heat treatment at four fields H_{dc} ($0 < H_{dc} < 126.5$ Oe).

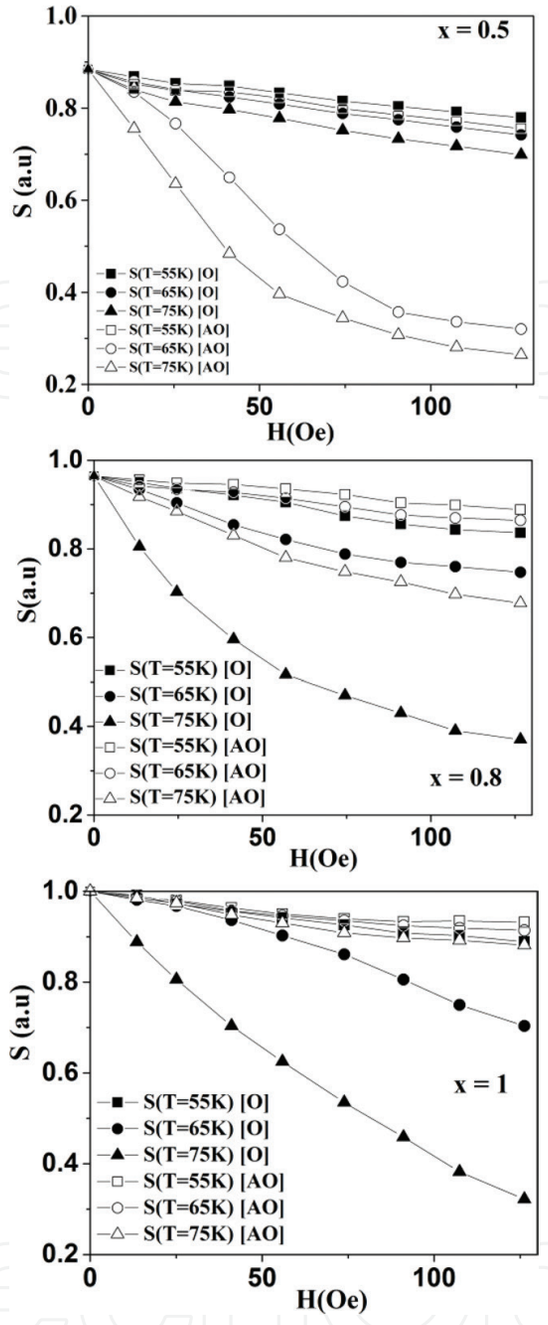

Figure 7. Shielding effect S of $(Y_{1-x}Sm_x)SrBaCu_3O_{6+z}$ as a function of the field H_{dc} and heat treatment at three different temperatures (55, 65 and 75 K).

3.4. Imaginary part of the AC magnetic susceptibility and irreversibility line

Looking to the imaginary part of the AC susceptibility χ″, of the sample $Y_{0.2}Sm_{0.8}SrBaCu_3O_{6+z}$ in **Figure 6(b)** for example, we can see that the width ΔT_p at half maximum of the transition in χ″(T) (see **Table 1**) was smaller in the samples [AO] at all H_{dc} and the peak T_p shifted less than in the sample [O]. **Figure 8** shows the field H_{dc} as a function of $t = T_p/T_c$ with an enhancement of the irreversibility line due to argon treatment for $x \geq 0.5$ [14]. The data can be analyzed with the help of following relation $H = K' (1 - t)^n$ [15]. Straight line plots were obtained when ln(H) was plotted against ln(1 – t) in **Figure 9**. For example, the value of K′ was estimated to be 1677

http://dx.doi.org/10.5772/intechopen.74354

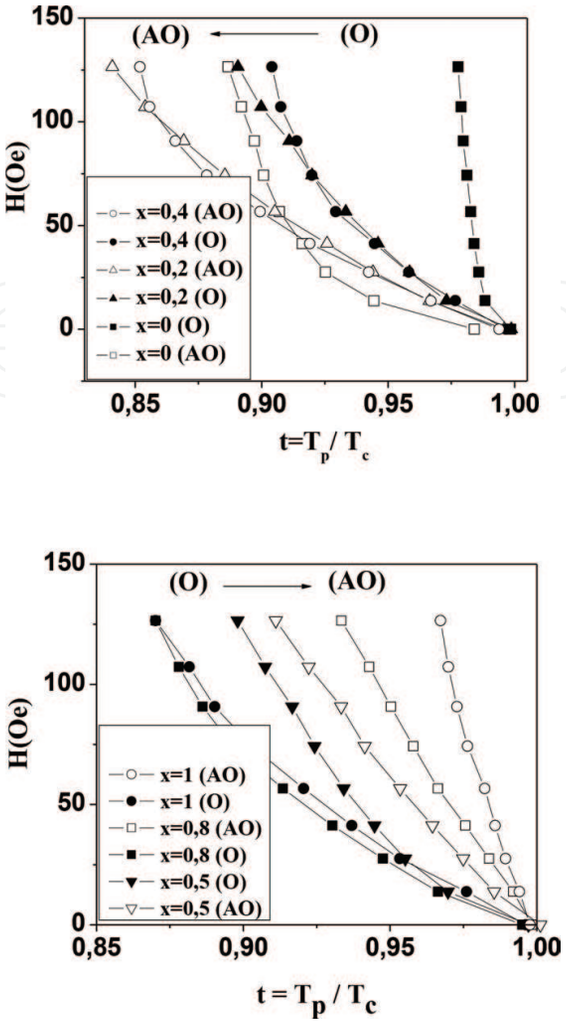

Figure 8. H as a function of $t = T_p/T_c$ and heat treatment of $(Y_{1-x}Sm_x)SrBaCu_3O_{6+z}$.

and 11,741 Oe, respectively, for the samples [O] and [AO] in $SmSrBaCu_3O_{6+z}$ (x = 1). K′ may be interpreted as the field necessary to reduce the intergranular critical current to zero in the limit of $T_p = 0$ K. We note that the argon treatment considerably increases the value of K′ and n, in **Table 1** and **Figure 10**, indicating an improvement in the pinning properties. The dashed line indicates the value n = 1.5 for the cuprites given by Miller et al. [15].

3.5. Resistivity

Figure 11 shows that the resistivity ρ(T) of the sample $SmSrBaCu3O_{6+z}$ increases with the temperature. For each temperature, ρ[AO] is superior to ρ[O]. For each x, T_c (ρ = 0) ≈ T_c (χ′) and for each heat treatment T_c (χ′) is superior to T_c (ρ = 0) by 2–3 K with T_p (χ″) ≈ T_c (ρ = 0). The linear part of ρ(T), in the normal state, follows the relationship $\rho = \rho_0 + \alpha T$, where ρ_0 is the residual resistivity extrapolated to T = 0 K and α is the slope dρ/dT. For example, the sample $SmBaSrCu_3O_{6+z}$ [O] has α = 1.8 (μΩ cm/K), ρ_0 = 242 (μΩ cm) and ρ297 K = 785 (μΩ cm). The treatment [AO] reduced considerably these parameters; in particular α[AO] = 0.9 (μΩ cm/K). This indicates a reduction of the interaction of carrier charges with phonons.

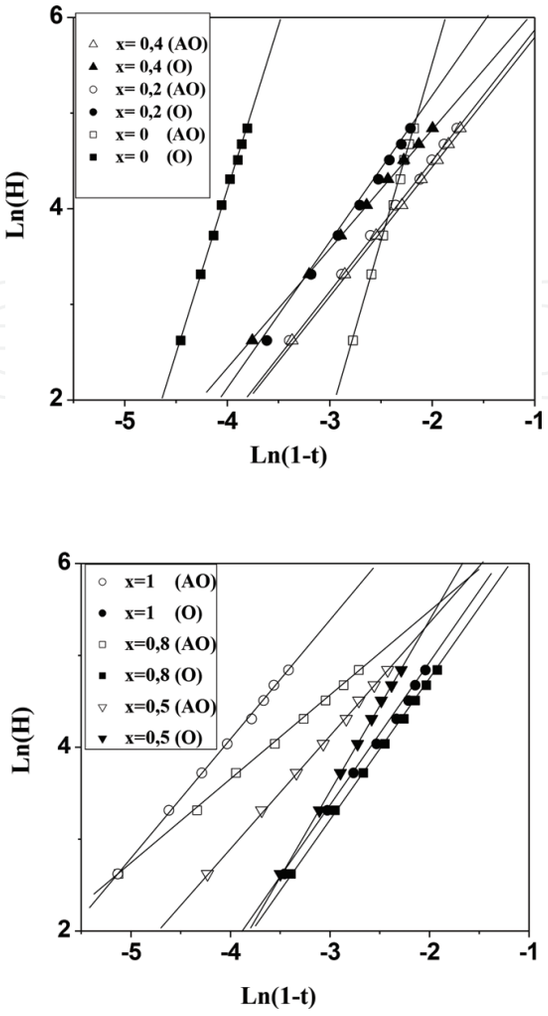

Figure 9. Ln(H) as a function of ln(1 − t) and heat treatment of $(Y_{1-x}Sm_x)SrBaCu_3O_{6+z}$.

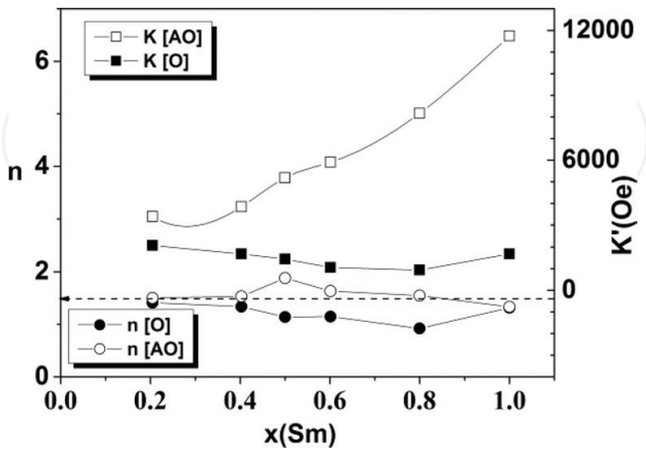

Figure 10. The field K′ and the exponent n as a function of x and heat treatment of $(Y_{1-x}Sm_x)SrBaCu_3O_{6+z}$.

http://dx.doi.org/10.5772/intechopen.74354

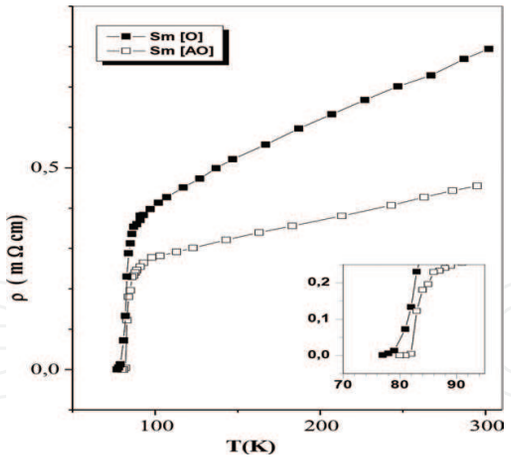

Figure 11. Resistivity ρ(T) of $SmBaSrCu_3O_{6+z}$ as a function of the temperature and heat treatment.

4. Discussions

We saw that the [AO] heat treatment increases the orthorhombic cleaving and eliminated some weak unidentified impurity peaks in **Figure 1(b)**. This indicates a good crystallization and an improvement of crystallographic quality of the samples [AO].

Our samples were prepared in 1 atm of oxygen. Our iodometry measurements show that the total oxygen constant was $6 + z = 6.94 \pm 0.04$ and do not change after the [AO] heat treatment. But for each x, T_c[AO] increased for $x \geq 0.4$. So this increase is not due to z but may lie in some other factor which governs the superconductivity in these samples.

When x increases from 0 to 1, T_c[O] decreases with ε. T_c[AO] decreases with the orthorhombicity ε until x = 0.2 and afterward it increases from 79 to 85 K in $SmSrBaCu_3O_{6+z}$ [AO], as shown in **Figure 12**. When x increases, the parameter b is constant but a (and c) increase

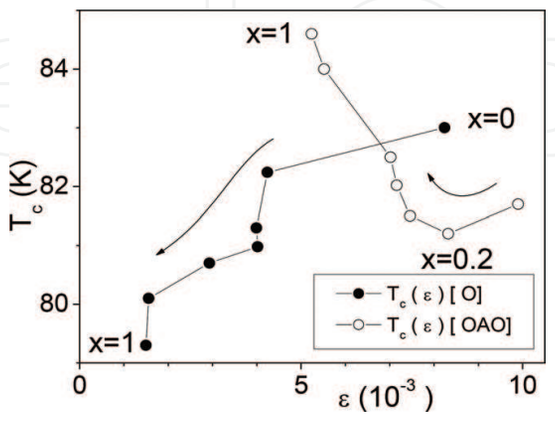

Figure 12. Variation of T_c as a function of the orthorhombicity ε and heat treatments of $(Y_{1-x}Sm_x)SrBaCu_3O_{6+z}$.

indicating an increase of the number of oxygen atoms by chain (NOC) along a axis with a decrease of ε (T_c[O]) from orthorhombic toward tetragonal structure in $SmSrBaCu_3O_{6+z}$ [O].

For each x, the [AO] treatment increases the orthorhombicity ε (for $0 \leq x \leq 1$) and T_c (for $x \geq 0.4$). For each x, the parameter a decreases and b increases after the [AO] heat treatment in the unit cell of **Figure 2**. Some oxygen atoms O(4) go to the vacant site O(5) along b axis. So the (NOC) and the anionic order in the basal plane increases leading to an increase of p_{sh} and T_c for $x \geq 0.4$ in **Figure 15**.

For each $x \geq 0.4$, the thermal parameter of the apical oxygen O(1) decreased from 2.02 to 0.27 $Å^2$ in the sample [AO] leading to a decrease of the cationic disorder; of Y (0.893 Å) (or Sm (0.965 Å) occupying some Ba (1.42 Å)/Sr (1.12 Å) sites along the c axis. Each sample [O] was heated in argon at 850°C. This action removes all the oxygen atoms from the structure and increases the atomic diffusion and the Y/Sm-Sr/Ba-Y/Sm order along c axis in the unit cell of **Figure 2**. In fact, the difference of bond valence (B.V.S.): V(Y)-V(Ba) = 0.77 in $YBa_2Cu_3O_{6.7}$ and 1.00 in $YBa_2Cu_3O_{6.32}$ indicate that the departure from reduced (6 + z) decreases the disorder of Y on the Ba site in $YBa_2Cu_3O_{6+z}$ [16]. So, the argon heat treatment decreases the disorder of Y/Sm on the Ba/Sr site. This is justified by the fact that impurity peaks seen in the [O] samples in **Figure 1(a)** disappeared after the [AO] heat treatment in **Figure 1(b)**.

Our results can be explained by the disorder of the oxygen in the basal plane, on the 0(4) and 0(5) sites along b and a axis, respectively, in **Figure 2**. This order enhanced the orthorhombic symmetry and increased the ratio (b − a)/(b + a). As seen on **Figure 13** when x increases, the interatomic distance d[Cu(1)—(Sr/Ba)] increases for both heat treatments in agreement with the fact that the crystallographic parameter c and the volume of the unit cell increases with x. For each x, the [AO] heat treatment decreases this distance for $x \geq 0.5$ (and increases it for $x < 0.5$). This decreases the distance d[Cu(1)—O(1)] and enhances the transfer of holes from the Cu(1)O chains to the superconducting planes $Cu(2)O_2$ via the apical oxygen O(1) resulting in an increase in the hole density p_{sh} and T_c for $x \geq 0.4$ in **Figure 15**. Such an increase leads to

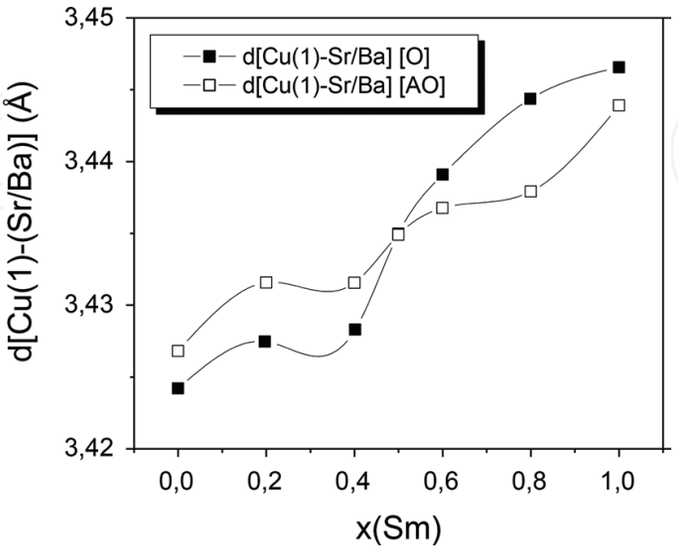

Figure 13. Interatomic distance d[Cu(1)—(Sr/Ba)] as a function of x and heat treatment in $(Y_{1-x}Sm_x)SrBaCu_3O_{6+z}$.

optimum superconducting properties and could account for the observed increase in T_c[AO] in agreement with the model of transfer of charges. This is justified by the fact that, when x increases, the parameter b is constant but a (and c) increase leading to an increase of the number of oxygen atoms by chain (NOC) along a axis with a decrease of ε (T_c[O]) from orthorhombic toward tetragonal structure in **Figure 12**.

When Sm ion occupies Ba (or Sr) site, the same amount of Ba (or Sr) cation is pushed into Y site. Sm is a three-valence ion. It increases the positive charge density around Ba (or Sr) site and the attractive force with oxygen anion. As a result, oxygen vacancies O(5) along the a-axis in the basal plane have higher chance to be filled. On the other hand, Ba^{+2} (or Sr^{+2}) in Y^{+3} (or Sm^{+3}) site decrease the attractive force with oxygen anion in Cu(2) plane. This increases the buckling angle Cu(2)—O(3)—Cu(2) along the a axis. When x increased from 0 to 1, the two changes of cation sites increase the parameter a. For each x, the [AO] heat treatment decreases the parameter a and increases b as shown in **Figure 2**. This increases the number of oxygen atoms by chain (NOC) along b axis leading to an increase of T_c with a decrease of the orthorhombicity ε for $x \geq 0.2$ as seen in **Figure 12**.

In the normal state, the heat treatment [AO] reduced considerably the linear resistivity parameters indicating a diminution of the interaction of carrier charges with phonons. $T_c(\chi')$ and $T_c(\rho = 0)$ were in good agreement.

For each $x > 0.5$, the [AO] heat treatment improved the shielding effect at all $T < T_c$ and for any applied field indicating an enhancement of the quality of the grains and intergranular coupling in the samples [AO]. Also for $x \geq 0.5$, an enhancement of the irreversibility line was noticed in the samples [AO] with an increase of the field K′ showing an improvement in the pinning properties. These results are justified by our XRD spectra, with Rietveld refinement, that showed an improvement of crystallographic quality of the samples [AO] in **Figure 1**.

The two arguments (cationic and anionic disorders) are justified here by the four remarkable correlations observed between $T_c(x)$, the volume of the unit cell V(x) in **Figure 14** and

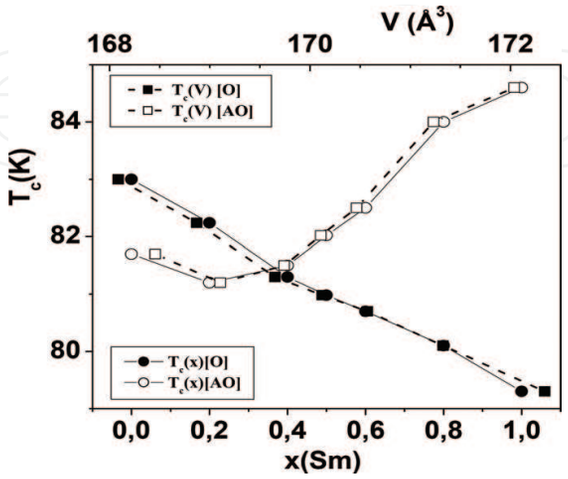

Figure 14. Correlation between T_c and the volume V of the unit cell as a function of x and heat treatment of $(Y_{1-x}Sm_x)SrBaCu_3O_{6+z}$.

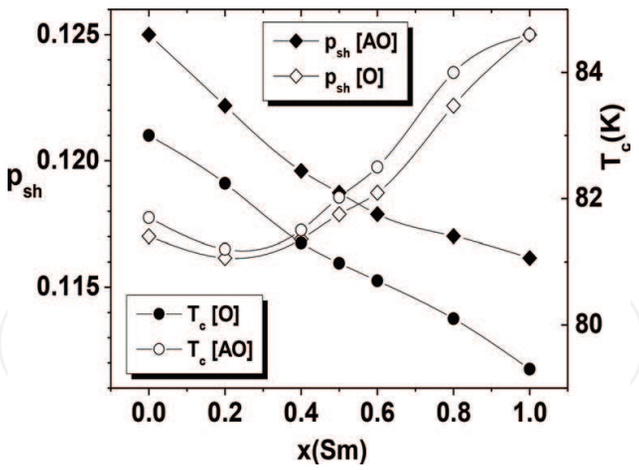

Figure 15. Correlation between p_{sh} and T_c as a function of x and heat treatment of $(Y_{1-x}Sm_x)SrBaCu_3O_{6+z}$.

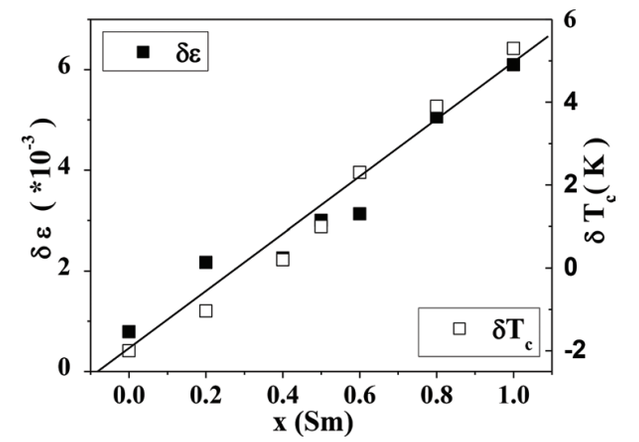

Figure 16. Correlation between $\delta T_c = T_c[AO] - T_c[O]$ and $\delta\varepsilon = \varepsilon[AO] - \varepsilon[O]$ as a function of x and heat treatment of $(Y_{1-x}Sm_x)SrBaCu_3O_{6+z}$.

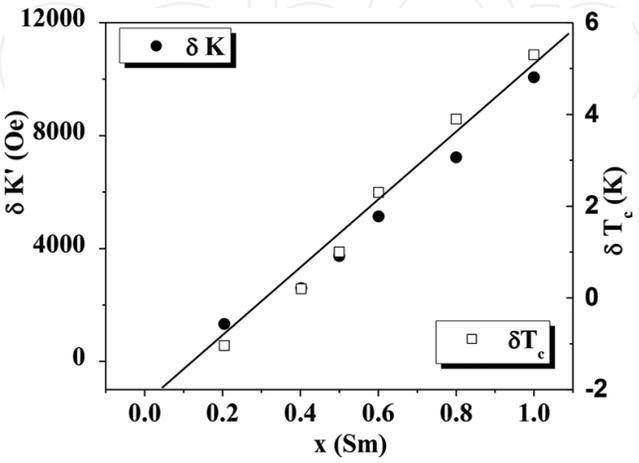

Figure 17. Correlation between δT_c and $\delta K'$ as a function of x and heat treatment of $(Y_{1-x}Sm_x)SrBaCu_3O_{6+z}$.

the number $p_{sh}(x)$ of holes by Cu(2)—O_2 superconducting planes in **Figure 15** (deduced from the undersaturation zone of the universal relation T_c/T_{cmax} (p_{sh}) [17]), and on the other hand, between $\delta T_c(x) = T_c[AO] - T_c[O]$ and $\delta\varepsilon(x)$ in **Figure 16** and between $\delta T_c(x)$ and $\delta K'(x)$ in **Figure 17**. So the structural, electrical and superconducting properties are correlated with the effect of argon heat treatment.

The increase or decrease in T_c must be related to the ionic size of the rare earth Sm, the variation of the Cu(1)-apical oxygen distance, hole density, anionic and cationic disorders, etc.

5. Conclusions

These studies indicate the optimization of the superconducting properties of the high-T_c superconductors $(Y_{1-x}Sm_x)SrBaCu_3O_{6+z}$ by a simple argon heat treatment. These results are a competition between oxygen disorder in basal plane and cationic disorder along c axis. In the samples [O], we are in the presence of a cationic disorder of Y/Sm on (Sr/Ba) sites that induced an anionic disorder of oxygen's chains in basal plane. Anionic order dominates in the samples [AO] in agreement with the previsions of [4, 5]. In the samples [AO], the remarkable improvement in the shielding effect (for $x > 0.5$) and the irreversibility line (for $x \geq 0.5$) are explained, respectively, by the improvement of the quality of the grains and intergranular coupling, and to the improvement of the pinning properties and crystallographic quality of these samples. The structural, magnetic and superconducting properties are correlated with the effect of argon heat treatment.

These results were explained by the effect of the ionic size of the rare earth, the decrease in d[Cu(1)—(Sr/Ba)]; the increase in cationic and chain oxygen ordering; the number of holes $p_{sh}(x)$ by Cu(2)—O_2 superconducting plans and in phase purity for the [AO] samples.

Author details

Abdelhakim Nafidi

Address all correspondence to: nafidi21@yahoo.fr

Laboratory of Condensed Matter Physics and Nanomaterials for Renewable Energy, University Ibn Zohr, Agadir, Morocco

References

[1] Tokura Y, Takagi H, Uchida S. A superconducting copper oxide compound with electrons as the charge carriers. Nature. 1989;**337**:345-347

[2] Cava RJ. Structural chemistry and the local charge picture of copper oxide superconductors. Science. 1990;**247**:656-662

[3] Raveau B, Michel C, Hervieu M, Grout D. Crystal Chemistry of High-Tc Superconducting Copper Oxides. Berlin: Springer-Verlag; 1991 (Ch. 1-3)

[4] Wada T, Suzuki N, Maeda A, Yabe T, Uchinokura K, Uchida S, Tanaka S. Preparation and properties of superconducting La1+xBa2-xCu3Oy ($0 \leq x \leq 0.5$) ceramics sintered in N2 gas atmosphere. Physical Review B. 1989;**39**(13):9126-9138

[5] Izumi M, Yabe T, Wada T, Maeda A, Uchinokura K, Tanaka S, Asano H. Structural properties of the superconductor LaBa2Cu3-yO7-z in the solid solution system La1+xBa2-xCu3-yO7-z. Physical Review B. 1989;**40**(10):6771-6786

[6] Nikolo M, Hermann AM. Magnetic Susceptibility of Superconductors and Other Spin SystemsHein RA, Francavilla TL, Leinberg DH, editors. New York: Plenum, 1991, p. 553

[7] Van der Pauw LJ. A method of measuring the resistivity and hall coefficient on lamellae of arbitrary shape. Philips Technical Review. 1958;**20**:220-224

[8] Braigue M, Nafidi A, et al. Correlation between enhanced T_c, orthorhombicity and the volume of the unit cell in argon preheated (Y1-xSmx)SrBaCu3O6+z. IEEE Transactions on Applied Superconductivity. 2009;**19**(3):2984-2987

[9] Rietveld HM. A profile refinement method for nuclear and magnetic structures. Journal of Applied Crystallography. 1969;**2**:65-71

[10] Hein RA, Francavilla TL, Leinberg DH, editors. Magnetic Susceptibility of Superconductors and Other Spin Systems. New York: Plenum; 1991

[11] Senoussi S. Review of the critical current densities and magnetic irreversibilities in high Tc superconductors. Journal de Physique III. 1992;**2**:1041-1257

[12] Nafidi A, Suryanarayanan R. Effect of heat treatment on the shielding properties of $NdSrBaCu_3O_{6+z}$. Physica Status Solidi (a). 1994;**146**:29-31

[13] Bellioua M, Nafidi A, Elkaaouachi A, Nafidi A, Suryanarayanan R. Enhancement of orthorhombicity, Tc, shielding and irreversibility line in argon preheated Sm(SrBa) Cu_3O_{6+z}. Physica C. 2002;**383**:183-190

[14] El Yakoubi EY, Nafidi A, et al. Correlation between enhanced Tc, AC magnetic irreversibility line and heat treatment in high Tc superconductors. IEEE Transactions on Applied Superconductivity. 2011;**21**(3):2727-2731

[15] Muller KA, Takashige M, Bednorz JG. Flux trapping and superconductive glass state in La_2CuO_{4-y}: Ba. Physical Review Letters. 1987;**58**(11):1143-1146

[16] Brown ID, Altermatt D. Bond-valence parameters obtained from a systematic analysis of the Inorganic Crystal Structure Database. Acta Crystallographica. 1985;**B41**(4):244-247

[17] Zhang H, Sato H. Universal relationship between Tc and the hole content in p-type cuprate superconductors. Physical Review Letters. 1993;**70**(11):1697-1699